EVIDENCE FOR ADSORBED HYDROCARBON INTERMEDIATES DURING THE INITIAL STAGES OF CO HYDROGENATION ON IRON

H.P. Bonzel and H.J. Krebs

Institut für Grenzflächenforschung und Vakuumphysik, Kernforschungsanlage Jülich, D-5170 Jülich, Germany

1. Introduction

Surface science techniques have been applied to the study of the surface properties of the transition metals Fe, Co, Ni and Ru /1-12/ and it is natural to extend the same approach to the study of Fischer-Tropsch synthesis (FTS) reactions on the same metal surfaces. However, reaction products in the adsorbed or gaseous phase apparently cannot be detected under vacuum conditions. Therefore, in order to utilize surface analytical techniques for the study of FTS, a combination of a surface analysis ultra-high vacuum system and an atmospheric reaction chamber has to be used, such as pioneered by Somorjai and coworkers /13, 14/.

In this paper we report on the use of such a combination apparatus of novel design with Auger electron (AES) and X-ray photoelectron spectroscopy (XPS) as analytical capabilities and a differential microreactor. The analysis of the reaction products is performed by gas chromatography (GC). Using this system we studied the hydrogenation of CO on polycrystalline iron foils and a Fe(110) single crystal at a total pressure of 100 kPa (= 1 bar ≅ 1 atm) /15/.

2. Experimental

The experimental system, sketched in Fig. 1, consisted of a stainless steel ultra-high-vacuum (UHV) chamber pumped by an ion pump, and an attached sample transfer system containing a small micro-reactor. The UHV chamber shown on the left hand side of Fig. 1 operates at a base pressure of 1×10^{-8} Pa. This system (Leybold-Heraeus) features an ion sputter gun for surface cleaning, an electron gun, X-ray source and high resolution electron spectrometer for Auger electron (AES) and photoelectron (XPS) spectroscopies, and a quadrupole mass spectrometer for residual gas analysis. The sample is either a polycrystalline iron foil about 0.1 mm thick, or a Fe(110) single crystal, with an active area of 0.35 cm^2. It is situated at a cutout portion of a stainless steel rod of 2 cm diameter. This rod serves as a transfer mechanism between UHV chamber, micro-reactor and atmosphere. The Fe sample can be heated resistively up to 1400 K in vacuum and about 900 K in 100 kPa of a H_2/CO mixture. The temperature of the sample is measured by a sheathed Chromel-Alumel thermocouple attached to the underside of the sample.

The micro-reactor of about 4 cm^3 total volume is a small section of the sample transfer system, Fig. 1. A mixture of CO and H_2 was passed continuously through this reactor at a rate of 50 cm^3/min. The partial pressure ratio of CO to H_2 was fixed by adjusting the individual flow rates of these two gases before entering the mixing stage. Partial pressure ratios of CO to H_2 from 1:100 to 1:4 could be easily chosen.

The transfer of the Fe-foil from the UHV system into the micro-reactor was accomplished by pulling the sample rod until the sample was located inside the reactor. The sample could be moved to the atmospheric loading position in a similar way, and also back into the UHV chamber. The transfer time from the reactor into the UHV position including pump-down to 10^{-6} Pa was 45 seconds. The sample rod itself is water cooled such that during heating of the Fe sample inside the micro-reactor no parts other than the sample and the tip of the thermocouple get hot. During the catalytic rate measurements the hydrocarbon products were analyzed by gas chromatography. A 0.5 cm^3 sample (loop volume) of the gas mixture was taken by the GC sample valve and passed over a 8 ft. Porapak Q column. The separated products were analyzed by a flame ionization detector.

The Fischer-Tropsch measurements were carried out in the following way: The

cleaned Fe sample was transfered from UHV into the micro-reactor where a steady state gas flow was already established. As soon as the sample came to a halt, the temperature was raised to the desired value as measured by the thermocouple. From this point on the time was measured and GC samples were taken periodically. At a later time the reaction was stopped by turning off the heating current. About 4 sec later the sample was transfered back to UHV for surface analysis by AES or XPS.

3. Results and Discussion

The measurements of FTS from CO and H_2 on Fe were carried out at a total pressure of 100 kPa (=1 atm) and CO/H_2 ratios of 1:100, 1:20 and 1:4. The temperature range investigated was 460-750 K. In all cases methane was the dominant product and its rate of formation time dependent. In order to check this time dependence, a series of GC reactivity measurements with a cycle of approximately 100 sec was carried out at the same temperature. Three examples of such curves are shown in Fig. 2 for a CO/H_2 ratio of 1:20 and different temperatures where the logarithm of the turnover number for methane is plotted as a function of time. These curves exhibit several interesting features: First, there is a strong rise in the methane rate of formation within the first 40-60 sec after reaching the reaction temperature. This rise signals the start of the reaction, and the apparent delay of about 30 sec prior to the rise (which is more obvious in a linear plot of rate versus time) represents the time it takes for the gas to flow from the reactor to the GC sampling valve. Second, there is a maximum in the rate of methane formation followed by a steady decline; both the position of the maximum and the slope of the decline depend on the temperature of the Fe-foil and the CO/H_2 ratio.

The occurence of the maximum in these curves of Fig. 2 is connected with the known pehnomenon of carbon accumulation on the Fe surface as a function of time /14,15/. The rate of carbon accumulation is faster, the higher the temperature or the higher the ratio of CO/H_2. However, the influence of the rate of carbon accumulation on the rate of CO hydrogenation is complicated due to different kinds of chemically bound carbon. We have measured the relative carbon concentration by XPS and present as an example the data in Fig. 3. This figure shows the carbon (1s) signal at different reaction times for similar experimental conditions as those of Fig. 2. In these experiments the Fe sample was moved into the micro-reactor for reaction for a short time, then into the UHV chamber for surface (AES or XPS) analysis, and back into the reactor for a continuation of the reaction.

The data in Fig. 3 illustrate the rapid increase in surface carbon concentration as a function of the reaction time and also a shift in the binding energy E_B of the C1s level from about 283.9 eV to 284.6 eV. Figure 4a shows the shift in E_B(C1s) versus time for a particular run at 530 K and CO/H_2 = 1:20. Figure 4b shows the corresponding integrated C1s peak area versus time. Note in Figs. 4a and 4b that the initial change in the plotted quantities, i.e. during the first 50 sec, is very rapid followed by a slower increase. It is tempting to associate this behaviour with the presence of different chemical carbonaceous species on the iron surface and with the rate of CH_4 formation.

Therefore we performed a number of experiments which were aimed at identifying the chemical nature of the carbonaceous surface phases after the CO/H_2 reaction. The procedure consists essentially in comparing the carbon Auger peak shapes and C1s binding energies of carbonaceous surface layers of known chemical origin (composition) with those of the surface phases generated by the hydrogenation of CO.

A total of three significantly different carbonaceous layers were observed after the hydrogenation reaction. Figure 5 shows the carbon Auger spectra of these three layers which we call the surface phases I, II and III, respectively. These spectra were obtained for CO/H_2 = 1:20. In comparing the Auger spectra of Fig. 5 one should in particular pay attention to the relative heights of the peaks labelled A, B and C. Other differences can be noted in the negative peak excursion at 270 - 285 eV. These, however, will not be referred to in this paper.

The carbon 1s spectra corresponding to the AES spectra in Fig. 5 showed different binding energies similar to those of Fig. 3. These measured C1s binding energies are listed in Table I together with the data for adsorbed acetylene, segregated carbidic and graphitic carbon.

Table I
C1s Binding Energies

Species	Binding Energy (eV)	
CO	285.9	produced in UHV
C_2H_2	283.9	
carbidic C	283.3	
graphitic C	285.0	
Phase I-CH_x	283.9	after reaction
Phase II	284.2	
Phase III	284.7	

Surface phase I

The C1s binding energies of this surface phase and chemisorbed molecular acetylene are identical within experimental error. This fact suggests that surface phase I is a heavily hydrogenated carbon layer. A comparison of Auger data, Fig. 6, shows, however, a substantial difference for surface phase I and acetylene. On the other hand, a very good simulation of the surface phase I Auger spectrum is obtained when a carbidic surface carbon produced in UHV by heating the sample to 720 K for about 2 min is exposed to C_2H_2 at 400 K for 5 min (2×10^{-5} Pa). It is likely that under these conditions some decomposition of C_2H_2 into CH species will occur /16,17/. We propose therefore that the surface phase I consists mainly of carbidic carbon and CH species.

Surface phase II

At first sight the Auger spectrum of surface phase II, Fig. 5, appears to be identical to the spectrum of carbidic carbon segregated under UHV conditions. However, this is not the case. Figure 7 shows both spectra for a direct comparison, and it can be noted that the peaks B and C of these two spectra are shifted against each other by about 2 eV. The reason for this shift is presumably bonded hydrogen in the case of the surface phase II, as expected from the shift of 0.9 eV for the C1s spectra of UHV carbidic carbon and surface phase II carbon (see Table I). The fact that some hydrogen is necessary in order to generate the Auger peak of surface phase II is illustrated by the following experiment: Fe(110) with segregated carbidic carbon was exposed to C_2H_2 at 475 (2×10^{-5} Pa, 5 min). The Auger spectrum taken subsequently is shown as trace (c) in Fig. 7 and it has features identical to those of the surface phase II spectrum.

The amount of bonded hydrogen in the surface phase II is presumably less than in the CH_x layer, mainly for two reasons: (1) There is no shape change in the Auger peak relative to carbidic carbon, only an energetic shift; (2) the procedure of simulating phase II involves an C_2H_2 exposure at higher temperatures (475 K compared to 400 K for CH_x simulation) facilitating the dehydrogenation of C_2H_2. The surface phase II can thus be characterized as a carbidic carbon layer with bonded hydrogen.

Surface phase III

The carbon Auger peak of the surface phase III has a great similarity with that of graphitic carbon /18,19/. Figure 8 shows an Auger trace of graphitic

carbon on Fe(110) which was segregated to the surface by heat treating the crystal in UHV (625 K, 25 min). Looking at the relative peak heights A, B and C one can notice the same sequence as in the spectrum of phase III. In a procedure equivalent to those discussed in the previous sections we can also produce a phase III type carbonaceous layer by exposing the Fe crystal with carbidic carbon to C_2H_2 at about 580 K (2×10^{-5} Pa, 20 min). The Auger peak of this layer is shown as trace (b) in Fig. 8. For comparison the phase III peak is included as trace (c). All three traces (a) - (c) have very similar shapes but from a closer inspection of the energetic positions of the peaks it is apparent that peak B for the traces (b) and (c) is shifted to lower kinetic energies relative to that of trace (a). Since both layers characterized by (b) and (c) are originating from gas phase reactions involving hydrogen, it is reasonable to assume that this peak shift is indicative of bonded hydrogen.

Hydrogenation behavior

An interesting observation was made when the various carbonaceous layers were subjected to hydrogen atmosphere at elevated temperature. It was seen that the CH_x layer and the hydrogen containing carbidic carbon layer (phases I and II, respectively) could be readily removed by hydrogenation but that the graphitic layer was quite inert towards H_2. An example of a hydrogenation of a mixed phase II/phase III layer is presented in Fig. 9. The total amount of carbon is seen to decrease but the binding energy shift from 284.4 eV to 284.9 eV indicates that carbidic carbon (phase II) is removed and graphitic carbon left behind on the surface.

The fast hydrogenation of surface phases I and II relative to the much slower removal of small amounts of graphitic carbon creates a possibility to separate the different phases in a mixed layer. Experiments of this kind showed that the total amount of carbon plotted for example in Fig. 4b could be broken up into a portion representing CH_x and carbidic carbon and a portion representing graphitic carbon. The first portion plotted versus time yields a maximum at about 30 - 50 sec similar to the maximum in Fig. 2. The second portion, graphitic carbon, increases steadily with time. We conclude that the maximum in reactivity is linked to the maximum in CH_x and carbidic carbon on the surface whereas the graphitic carbon acts as an inhibitor on the methanation as well as the Fischer-Tropsch reaction.

4. Conclusions

1. Layers of (UHV segregated) carbidic and graphitic carbon, molecularly adsorbed CO and C_2H_2 can be fairly well characterized by their respective carbon Auger peak fine structure and C(1s) binding energies.

2. Carbonaceous layers deposited by the CO hydrogenation reaction at 1 bar were analyzed by AES and XPS and could be classified by a comparison of carbon Auger line shapes and C(1s) binding energies with those of layers of known chemical composition.

3. A carbonaceous layer of particular interest formed in the initial phase of CO hydrogenation on Fe(110) was found to correspond to heavily hydrogenated carbidic carbon, most likely a CH_x phase. This phase is suggested to consist mostly of CH radicals.

4. The CH_x phase and carbidic carbon can be easily removed from the surface by hydrogenation; graphitic carbon is quite stable towards hydrogen at 1 bar and elevated temperatures.

5. The maximum in the time dependent methanation rate correlates with the maximum in CH_x and carbidic carbon; these latter species are important intermediates for the formation of methane and probably higher molecular weight products.

References

/1/ K. Kishi and M.W. Roberts, J. Chem. Soc. Faraday Trans. I 71 (1975) 1715

/2/ R.W. Joyner and M.W. Roberts, J. Chem. Soc. Faraday Trans. I 70 (1974) 1819

/3/ K.Y. Yu, W.E. Spicer, I. Lindau, P. Pianetta and S.F. Lin, Surface Sci. 57 (1976) 157

/4/ C.R. Brundle, IBM J. Res. Develop 11 (1978) 235

/5/ G. Brodén, G. Gafner and H.P. Bonzel, Appl. Phys. 13 (1977) 333

/6/ T.N. Rhodin and C.F. Brucker, Solid State Comm. 23 (1977) 275

/7/ W. Erley and H. Wagner, Surface Sci. 74 (1978) 333

/8/ G. Wedler, K.G. Colb, G. McElhiney and W. Heinrich, Appl. Surface Sci. 2 (1978) 30

/9/ K.A. Prior, K. Schwaha and R.M. Lambert, Surface Sci. 77 (1978) 193

/10/ R. Ku, N.A. Gjostein and H.P. Bonzel, Surface Sci. 64 (1977) 465

/11/ H.P. Bonzel and T.E. Fischer, Surface Sci. 51 (1975) 213

/12/ K.J. Singh and H. Grenga, J. Catal. 47 (1977) 328

/13/ B.A. Sexton and G.A. Somorjai, J. Catal. 46 (1977) 167

/14/ D.J. Dwyer and G.A. Somorjai, J. Catal. 52 (1978) 291 and J. Catal. 56 (1979) 249

/15/ H.J. Krebs, H.P. Bonzel and G. Gafner, Surface Sci. (to be published)

/16/ C.F. Brucker and T.N. Rhodin, J. Catal. 47 (1977) 214

/17/ T.N. Rhodin, C.F. Brucker and A.B. Anderson, J. Catalysis (to appear)

/18/ J.P. Coad and J.C. Rivière, Surface Sci. 25 (1971) 609

/19/ C.C. Chang, Surface Sci. 25 (1971) 53

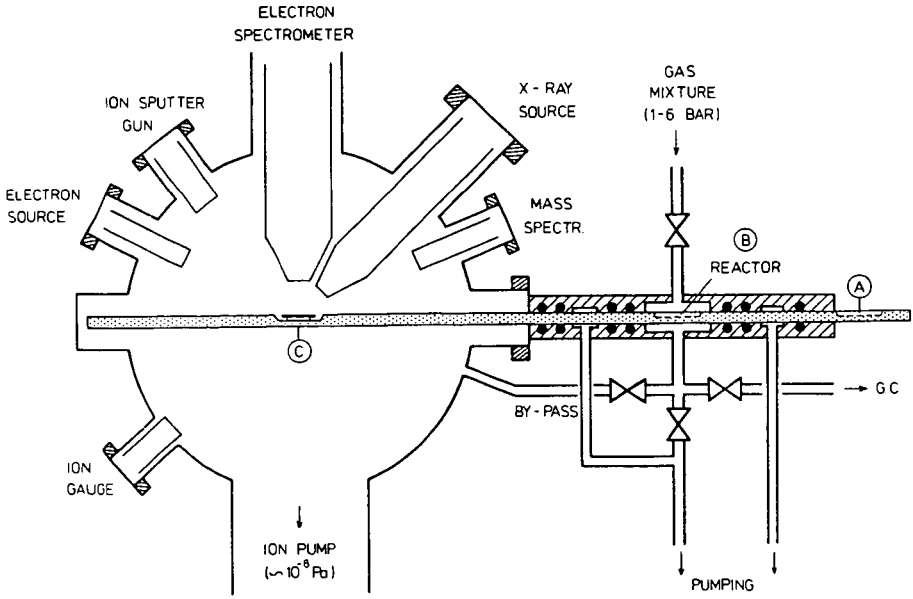

Figure 1: Schematic of UHV apparatus with attached sample transfer system and micro-reactor for catalytic rate measurements. The sample, located at the surface analysis position "C" in the center of the UHV chamber, can be moved by pulling the stainless steel rod, to the position "B" (reactor for chemical reaction) or position "A", the atmospheric loading position.

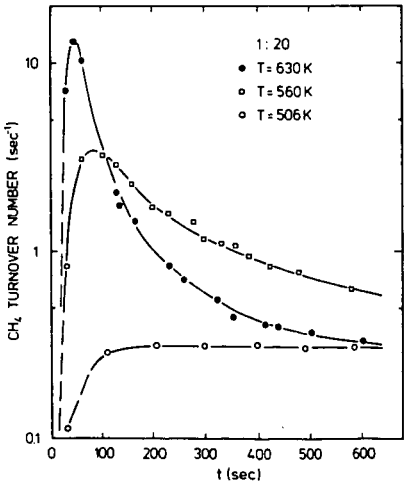

Figure 2: Semilog-plot of methane turnover number versus time for a CO/H_2 ratio of 1:20.

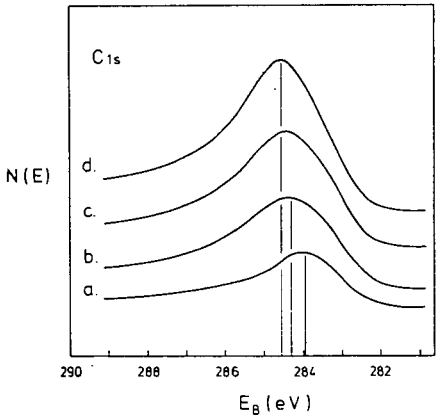

Figure 3: Carbon 1s XPS data after reaction, CO/H_2 = 1:20, T = 530 K, reaction times a) 3 sec, b) 23 sec, c) 83 sec and d) 600 sec. Note shift in maximum.

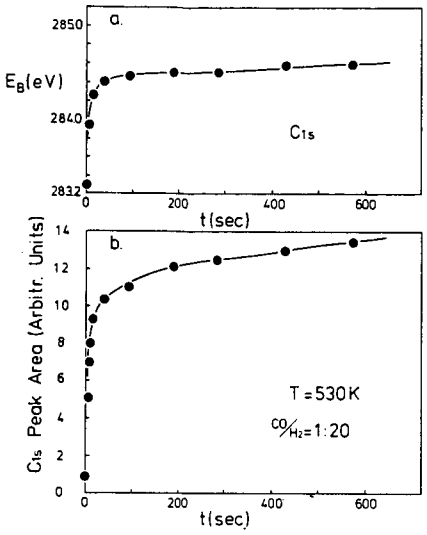

Figure 4: Same reaction data as in Fig. 3. (a) C1s binding energy as a function of reaction time. (b) Integrated C1s peak area (as a measure of surface carbon concentration) versus reaction time.

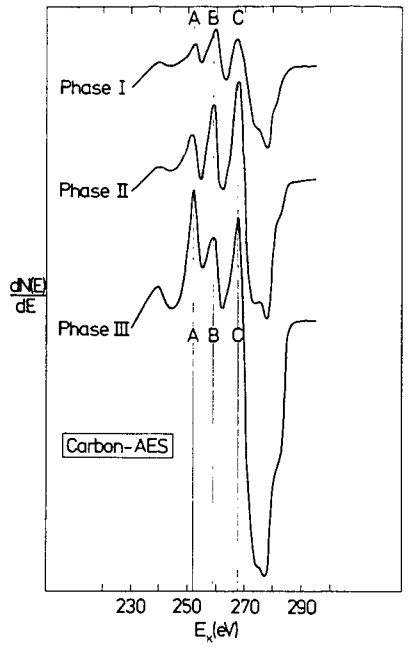

Figure 5: Carbon Auger spectra of the three carbonaceous surface phases formed after the CO/H_2 reaction at 1 bar and CO/H_2 = 1:20. Reaction conditions: Surface phase I - T = 565 K, t = 15 sec; surface phase II - T = 615 K, t = 15 sec; surface phase III - T = 615 K, t = 90 min.

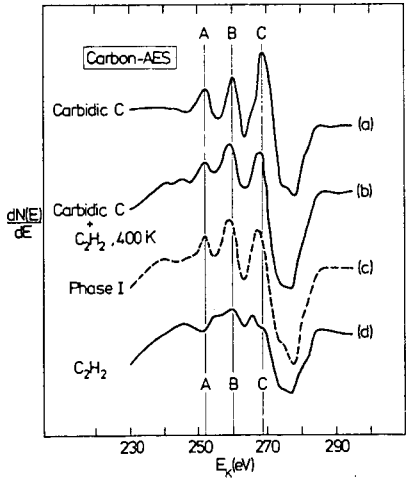

Figure 6: Carbon Auger spectra. (a) After heating the Fe(110) crystal in UHV at 720 K for about 3 min; (b) after exposure of the carbidic carbon on Fe (110) to 2×10^{-5} Pa C_2H_2 for 5 min at 400 K; (c) after reaction at 1 bar; (d) after exposing the clean Fe(110) crystal to C_2H_2 at room temperature (2×10^{-5} Pa, 5 min).

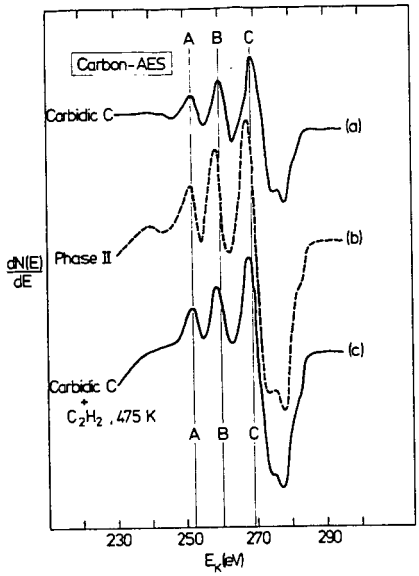

Figure 7: Carbon Auger spectra. (a) Fe(110) crystal was heated in UHV to 720 K for about 3 min; (b) after CO/H_2 reaction at 1 bar; (c) after exposing the surface produced under (a) to C_2H_2 at 475 K (2×10^{-5} Pa, 5 min).

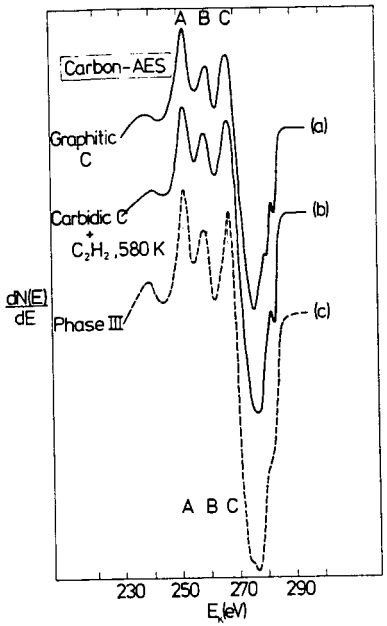

Figure 8: Carbon Auger spectra. (a) Fe(110) crystal was heated in UHV to 625 K for about 25 min; (b) after exposure of the Fe surface to C_2H_2 at 580 K (2×10^{-5} Pa, 20 min); after CO/H_2 reaction at 1 bar.

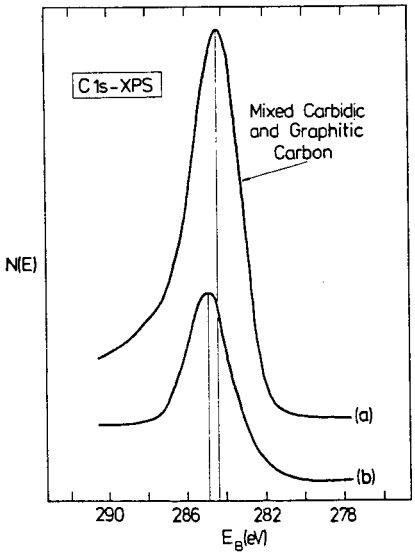

Figure 9: C1s spectra. (a) After CO/H_2 reaction at 1 bar and 630 K (CO/H_2 = 1:20, 10 min reaction time); (b) after hydrogenation of the surface under (a) at 1 bar, 630 K for 60 min.